Analysis of Equatorial X-Ray Diffraction Patterns from Muscle Fibers: Factors that Affect the Intensities

S. Malinchik and L. C. Yu

Laboratory of Physical Biology, National Institute of Arthritis, Musculoskeletal and Skin Diseases, National Institutes of Health, Bethesda, Maryland 20892

ABSTRACT Previously we have shown that cross-bridge attachment to actin and the radial position of the myosin heads surrounding the thick filament backbone affect the equatorial x-ray diffraction intensities in different ways (Yu, 1989). In the present study, other factors frequently encountered experimentally are analyzed by a simple model of the filament lattice. It is shown that the ordering/disordering of filaments, lattice spacing changes, the azimuthal redistributions of cross-bridges, and variations in the ordered/disordered population of cross-bridges surrounding the thick filaments can distinctly affect the equatorial intensities. Consideration of Fourier transforms of individual components of the unit cell can provide qualitative explanations for the equatorial intensity changes. Criteria are suggested that can be used to distinguish the influence of some factors from others.

INTRODUCTION

Equatorial x-ray diffraction patterns of skeletal muscle have been widely used to study mass distributions in muscle cells for several decades. It has been established that the equatorial diffraction patterns originate from the hexagonal arrays of the interdigitating thick and thin filaments. The reflection intensities provide information about the density profiles of the filaments (projected onto a plane perpendicular to the fiber axis). This is equivalent to studying the integrated densities in a thick cross section of the sarcomeres.

The strongest reflections of the diffraction pattern from skeletal muscle are found along the equator, particularly the [1,0] and [1,1] reflections. With advances in detection technology (e.g., position-sensitive proportional counters and imaging plates) and the availability of synchrotron radiation, the time resolution for recording equatorial x-ray diffraction patterns has reached the sub-millisecond range even for single muscle fibers (diameter ~80 μm). Thus, during biochemical and mechanical interventions, e.g., isotonic shortening (Podolsky et al., 1976; Huxley, 1978; Yagi et al., 1993), force redevelopment (Huxley et al., 1983; 1988; Irving et al., 1992), tetanus rise (Cecchi et al., 1991), and the release of caged compounds (Poole et al., 1988), cross-bridge behavior may be followed with millisecond or sub-millisecond time resolution.

Changes in the intensities of the [1,0] and [1,1] reflections (I_{10} and I_{11}) have been correlated with changes in the fraction of cross-bridges attached to actin in specific physiological states (Huxley, 1968; Yu et al., 1979; Brenner et al., 1984; Brenner and Yu, 1985). In previous analyses, (Lymn and Cohen, 1975; Haselgrove et al., 1976; Lymn, 1978; Yu, 1989, Irving and Millman, 1989) model calculations showed that there are other factors which could affect the equatorial diffraction, e.g., the angle of cross-bridge attachment to actin and the radial position of the myosin heads surrounding the thick filament backbone. However, the interpretation of equatorial reflections is not straightforward. Additional factors such as ordering/disordering of filaments, lattice spacing changes, azimuthal redistributions of cross-bridges and variations of the ordered/disordered population of cross-bridges surrounding the thick filaments are frequently encountered in experiments. The effects of these factors are illustrated here and suggestions are made for a few criteria that can distinguish one factor from another. Preliminary results have been reported previously (Malinchik and Yu, 1993).

MATERIALS AND METHODS

According to diffraction theory, the scattering intensity in the equatorial direction depends only on the projections of filaments onto the equatorial plane. In modeling of low-angle diffraction patterns (limited by reciprocal radius <1/100 Å, the spacing of the [3,0] equatorial reflection), we assume that projections of both myosin and actin filaments are cylindrically symmetrical. This assumption neglects the fine structures of the filaments, the three-stranded nature of the thick filament backbone and ninefold symmetry of the myosin head helix in axial projection. However, at resolution <100 Å, the fine structures of actin and myosin filaments as well as the individual myosin heads are invisible. Our simplifications are therefore reasonable.

In a muscle cell, the filaments form a hexagonal array with the thick filaments at the lattice points and the thin filaments at the trigonal points (Squire, 1981). The unit cell consists of one thick and two thin filaments.

For each equatorial reflection with the index [*h*,*k*], the Fourier transform of the unit cell is

$$F^{hk} = F^{hk}_{Thick} + 2F^{hk}_{Thin} \cos\left[\frac{2\pi}{3}(h + k)\right]$$

The corresponding intensity is

$$I^{hk} = |F^{hk}|^2$$

where F^{hk}_{Thick} and F^{hk}_{Thin} are cylindrically symmetrical Fourier transforms of

Received for publication 15 September 1994 and in final form 7 February 1995.

Address reprint requests to Dr. Sergey Malinchik, LPB/NIAMS, National Institutes of Health, Bldg. 6, Rm. 425, Bethesda, MD 20892. Tel.: 301-496-6723; Fax: 301-402-0009; E-mail: smalinch@helix.nih.gov.

0006-3495/95/05/2023/09 $2.00

TABLE 1 Fourier transforms associated with reflection [h,k] originated from thick and thin filaments

Reflection index [h,k]	Reciprocal radius (R)	F^{hk}	Number of equatorial reflections
1,0	a*	$F_{Thick} - F_{Thin}$	6
1,1	3a*	$F_{Thick} + 2F_{Thin}$	6
2,0	2a*	$F_{Thick} - F_{Thin}$	6
2,1	$\sqrt{7}$a*	$F_{Thick} - F_{Thin}$	12
3,0	3a*	$F_{Thick} + 2F_{Thin}$	6
2,2	$\sqrt{3}$a*	$F_{Thick} + 2F_{Thin}$	6
3,1	$\sqrt{13}$a*	$F_{Thick} - F_{Thin}$	12

$a^* = 2/(\sqrt{3}a)$ is the size of the reciprocal lattice; a is the size of the unit cell and also the distance between nearest thick filaments.

the projections of thick and thin filaments, respectively, at the $[h,k]$ spacings. The cosine term accounts for symmetrical displacements of two thin filaments in the unit cell with the thick filament at the origin. Table 1 shows the combinations of F^{hk}_{Thick} and F^{hk}_{Thin} and corresponding reciprocal radii (R) for the first seven equatorial reflections.

The thick filament structure is assumed to consist of a backbone described by a homogeneous cylinder with a radius equal to 90 Å, and with cross-bridges surrounding the backbone. Each cross-bridge is modeled by a single cylinder consisting of seven overlapping spheres in a straight line with 20 Å between the centers and a radius of 20 Å for each sphere (Miller and Treager, 1972). The spatial configuration of cross-bridges surrounding the thick filament is described in terms of the distance between the center of the cross-bridge and the center of the thick filament, r_c; and two angles, the axial angle α, and the azimuthal angle β, as shown in Fig. 1 *a*. The density distribution of the cross-bridge halo is obtained as a result of azimuthal averaging of a single cross-bridge projection. (The S2 connection between myosin S1 and the filament is flexible and of low mass. Thus the diffraction from this structure will be minimal and is treated here as a gap between S1 and the filament backbone.)

The thin filament structure is represented by a homogeneous cylinder with a radius of 55 Å. Attachment of the cross-bridges, which are centered around the thin filament, is also described in terms of two spatial angles ϕ_{att} and ψ_{att} (see Fig. 1 *b*).

The Fourier transform of the myosin filament projection, $F_{Thick}(R)$, is the sum of the transforms of the filament backbone, $F_B(R)$, and the cross-bridge halo, $F_H(R)$:

$$F_{Thick}(R) = F_B(R) + F_H(R)$$

where R is the reciprocal radius. For the backbone represented by a cylinder of radius r_B with a molecular weight of W_B (Vainstein, 1966):

$$F_B(R) = W_B \frac{J_1(2\pi R r_B)}{\pi R r_B}$$

where the transform of the cylinder is divided by the term πr_B^2 to normalize the mass of the cylinder to the unit. The cylindrically symmetrical transform of the cross-bridge projection (the cross-bridge is represented by seven spheres of radius r_0) is

$$F_H(R) = W_H \cdot FORM(U) \cdot \frac{\sum_{j=1}^{7} J_0(2\pi R r_j)}{7}$$

where

$$FORM(U) = \frac{3(\sin U - \cos U)}{U^3};\ U = 2\pi R r_0$$

is the structural factor of the projection of a single sphere of radius r_0. W_H is the molecular weight of the whole cross-bridge halo. Transform of the cross-bridge projection is also normalized to the unit mass by dividing by 7. r_j is the distance from the origin of the unit cell (i.e., the center of the thick filament backbone) to the center of the projection of each sphere in the cross-bridge:

$$r_j = \sqrt{r_c^2 + (l_j \cos\alpha)^2 + 2\, r_c l_j \cdot \cos\alpha \cdot \cos\beta}$$

l_j is the distance along the cross-bridge axis of the j^{th} sphere from the center of the cross-bridge (= distance between spheres × the number of the sphere from the center).

The Fourier transform of the thin filament projection, $F_{Thin}(R)$, is the sum of the transforms of the thin filament itself, $F_A(R)$, and the attached cross-bridges, $F_{att}(R)$:

$$F_{Thin}(R) = F_A(R) + F_{att}(R)$$

$F_A(R)$ and $F_{att}(R)$ are calculated in the same manner as shown above for the thick filament.

The molecular weights W_B, W_H, and W_A per half sarcomere at full overlap are proportional to the molecular weights of the thick filament backbone, the cross-bridges surrounding the backbone, and the overlapping part of the thin filament including regulatory proteins. Based on the available data (Squire, 1981) we assume that without any attached cross-bridges present, $W_B \approx 36 \times 10^3$ kDa (150 myosin molecules × 240 kDa, weight of the rod part of the molecule); $W_H \approx 40 \times 10^3$ kDa (150 myosin molecules × (2 × 130 kDa) – weight of two S1); $W_A \approx 16 \times 10^3$ kDa (weight of overlapping part of the thin filament ~6700 Å long). W_{att} is defined as the mass of the attached cross-bridges that surround the thin filament. Whenever W_{att} is >0, it is subtracted from W_H. However, due to the stoichiometry of the unit cell, the gain in W_{att} is equal to one-half of the loss in W_H (On average, mass of cross-bridges from one thick filament is redistributed between two thin filaments in the unit cell).

Taking into account disordering effects (random isotropic displacements), the structure factor of the corresponding disordered component of

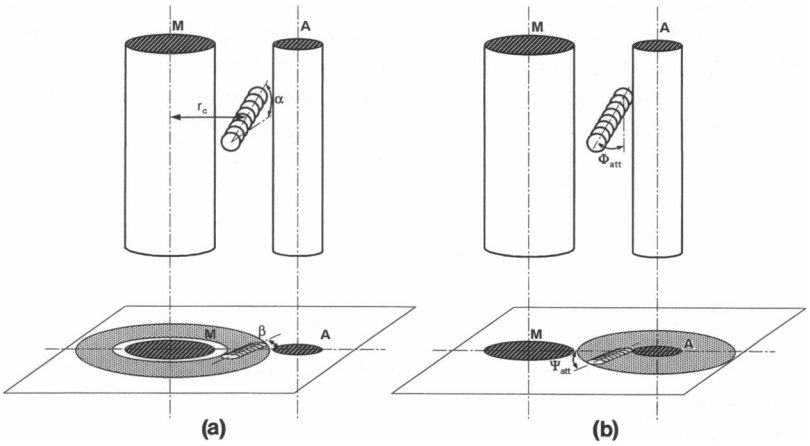

FIGURE 1 The models of thick and thin filaments used for Fourier transform calculations. The thick filament backbone is represented by a uniform cylinder 180 Å in diameter. Myosin cross-bridges are represented as cylindrical rods 160 Å in length. They are described in terms of seven overlapped spheres with a radius of 20 Å. The configuration of each cross-bridge is described by the distance of center of mass from the filament center r_c and two spherical angles α and β (*a*). The actin filament is represented by a uniform cylinder of 110 Å in diameter. The configuration of cross-bridges attached to actin is described by two spherical angles ϕ_{att} and ψ_{att}. (*b*) ϕ_{att} is the angle of attachment. Axial projections of thick and thin filaments, which were used to calculate equatorial diffraction patterns, are shown. In (*a*) cross-bridges are thick filament-centered; in (*b*) they are attached to and centered around the thin filament.

the unit cell is multiplied by a "temperature" factor (Vainstein, 1966):

$$D = \exp(-2\pi^2\Delta^2R^2)$$

where Δ is the root mean square (rms) isotropic displacement of the corresponding component, and R is the distance from the origin in reciprocal space.

The Fourier transforms and the intensities of the first seven reflections were calculated for each set of parameters. To compare the calculated results with the experimental data, a Lorentzian factor was included (dividing the calculated intensities by the radius in reciprocal space; Sherwood, 1976). In addition, the calculated intensities of [2,1] and [3,1] reflections were multiplied by a factor of 2, because there are twice as many reflection planes with these two indices as the others listed in Table 1. The calculations and graphics were performed on a personal computer using MLAB software for scientific modeling (Civilized Software, Inc., Bethesda, MD).

RESULTS

The influence of different parameters on the equatorial diffraction pattern was studied. In most cases we started with a "basic" model that gives a diffraction pattern with $I_{10} \approx I_{11}$. It has the following parameters: the cylindrical backbone of the thick filament is 180 Å in diameter and has a total relative weight of $W_B = 36$, cross-bridge halo surrounding backbone has a total relative weight of $W_H = 33$, and a radial density distribution calculated from a single cross-bridge with the following values: $r_c = 135$ Å, $\alpha = 0°$, and $\beta = 70°$. The thin filament is represented by a cylinder of 110 Å in diameter with a relative weight of $W_A = 14$. (The relative weights of the cross-bridge halo and thin filament were reduced from those calculated in Materials and Methods to make I_{10} equal to I_{11}. This may reflect the fact that these components are disordered in muscle and effectively have lower relative weights.)

In the following results, emphasis is placed on changes in the intensities I_{10} and I_{11}.

The first two models, presented bellow, show that our calculations are consistent with earlier results of Lymn (1978) and Yu (1989), although absolute values differ because the models are slightly different.

Changing the fraction of attached cross-bridges

Cross-bridges are assumed to move from the thick filament region, to surround the actin and become attached at angles $\phi_{att} = 45°$ and $\psi_{att} = 60°$. The increase in the fraction of cross-bridges bound to actin filament results in the well-known reciprocal change in I_{10} and I_{11} (Fig. 2 *a*) (Lymn, 1978; Yu, 1989). The axial attachment angle, ϕ_{att}, with constant fraction of attachment (100% in our case), affects the slopes of the curves in Fig. 2 *b*. Similar effects are seen by changing the slew angle of attachment ψ_{att}.

Radial movement of cross-bridge halo

The distance from the center of the thick filament to the center of the radial distribution of cross-bridges, r_c, is allowed to vary over a 30-Å range while the spatial configuration of cross-bridges remains constant (Fig. 2 *c*). As found previously (Yu, 1989), I_{10} is far more sensitive than I_{11} to the radial movement of the cross-bridge halo.

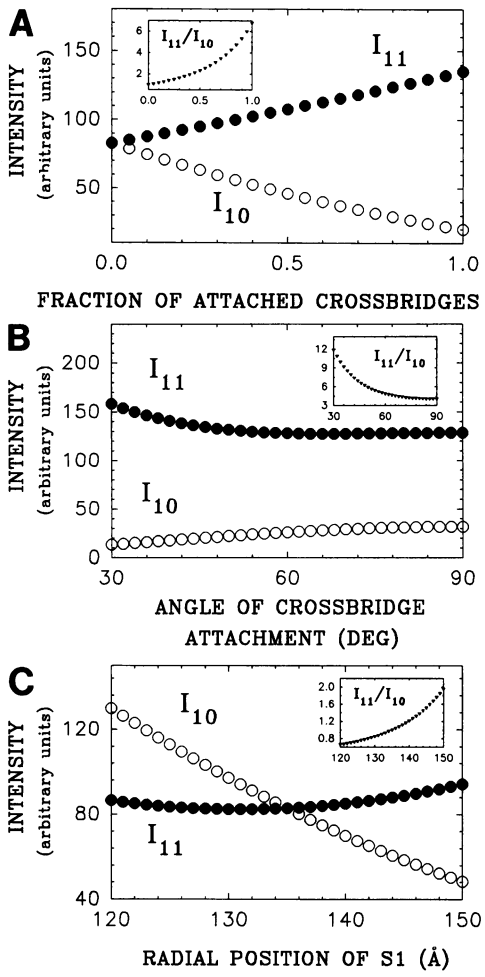

FIGURE 2 (*a*) Variation of fraction of attached cross-bridges. The model consists of two different populations of cross-bridges. One fraction of cross-bridges surrounds the thick filaments ($r_c = 135$ Å, $\alpha = 0°$, and $\beta = 70°$). The second fraction of cross-bridges is attached to and centered around the thin filament. The change of I_{10} and I_{11} intensities with changing number of attached cross-bridges is showed. *Inset*: calculated I_{11}/I_{10} ratio. (*b*) Different angles of attachment. All cross-bridges are assumed to be attached to the thin filaments. The axial attachment angle, ϕ_{att}, is changed in the range from 30° to 90° ($\psi_{att} = 60°$, constant). (*c*) Radial movement of cross-bridge halo. The cross-bridge center, r_c, moves away from the thick filament center in range from 120 to 150 Å. Configurations of individual cross-bridges is constant. The characteristic feature of this model is the high sensitivity of I_{10}, while I_{11} does not change.

The following models deal with conditions not considered previously.

Ordering-disordering effects

1) If the thick filaments as a whole including cross-bridges are allowed to undergo isotropic random displacements from their ideal lattice positions (disorder of the first type; Vainstein, 1966), the projected thick filament density becomes smeared and the effective size of the filaments increases. Both I_{10} and I_{11} decrease with the increase of disordering of thick filaments (rms isotropic displacement of filaments, Δ, changes from 0 to 30 Å). I_{10} however, is much more sensitive, and hence the I_{11}/I_{10} ratio increases (Fig. 3 *a*).

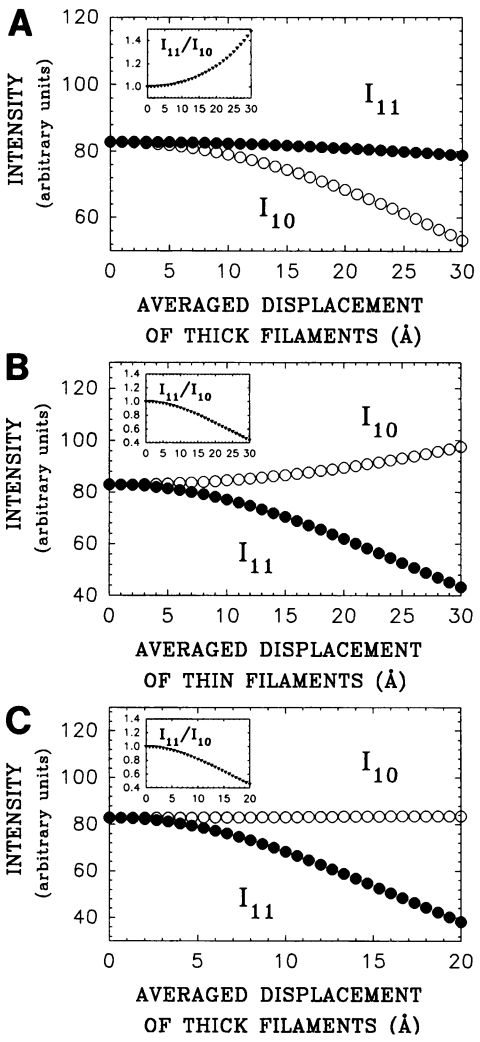

FIGURE 3 Ordering-disordering effects of filaments. (*a*) The thick filaments with cross-bridges are assumed to be subjected to random isotropic displacement from their lattice positions (disorder of the first type with Gaussian distribution of thick filament centers). The configurations of individual filaments and cross-bridges are constant. Both I_{10} and I_{11} decrease with thick filaments disordering but I_{10} is much more sensitive. (*b*) The thin filaments are assumed to be subjected to random displacement from their idealized positions in the lattice (disorder of the first type with Gaussian distribution of thin filament centers). I_{10} and I_{11} change in a reciprocal way with increasing disorder. (*c*) Both thick and thin filaments are displaced randomly (in the same way as in (*a*) and (*b*)) and in the process thin filaments have rms displacement larger by a factor of 1.6 ($\Delta_{Thin} = 1.6\Delta_{Thick}$).

2) Thin filament positions are allowed to fluctuate in the same manner and in the same range (Δ changes from 0 to 30 Å) as described above for the thick filaments. This changes the situation considerably: I_{10} increases with disorder, while I_{11} decreases (Fig. 3 *b*).

3) When both thick and thin filaments are allowed to undergo a "temperature" disorder of the same magnitude, we get a mixture of the two examples shown above. Since the thin filaments are less massive than the thick filaments, it is expected that the amplitudes of random displacements for the thin filaments will be larger than those for the thick filaments. In Fig. 3 *c* the average displacements of thin filaments are larger by a factor of 1.6 than those for thick filaments. For the [10] reflection the disordering effect of the thin filaments is balanced out by that of the thick filaments and the intensity of this reflection is hardly affected by isotropic disorder. However, the intensity of the [11] reflection is considerably reduced because the disordering effects in both filaments accumulate.

Lattice effects

It has been observed that a wide range of conditions can cause changes in the lattice spacing, particularly in the skinned fibers. Frequently, changes in intensities accompany changes in lattice spacings. If one assumes that as the lattice expands/shrinks, the filaments and the surrounding halo of myosin heads are unaffected (i.e., the changes in lattice spacing only changes the separation between the filaments), substantial changes in I_{10} and I_{11} could accompany the changes in lattice spacing (Fig. 4). Both I_{10} and I_{11} increase with the swelling of the lattice, but because the increase in I_{10} is greater than I_{11}, the I_{11}/I_{10} ratio decreases.

Azimuthal uniformity

The azimuthal mass distributions of all of the models presented above is assumed to be uniform. Now we consider effects of nonuniform azimuthal distributions. Two main types of sixfold symmetry in the azimuthal distribution of cross-bridges are studied.

1) cross-bridges are assumed to be concentrated along lines joining myosin-actin centers, [1,1] lines. For simplicity, to control the degree of nonuniformity in the cross-bridge density distribution, the whole population of cross-bridges is divided into two fractions: cross-bridges of the first fraction are distributed homogeneously around the thick filament backbone while the cross-bridges of the second fraction are located along the [1,1] lines. The cross-bridges in both populations have the same orientations with respect to the thick filament and are located at the same distance from the center of thick filament. The ratio of cross-bridges in these two fractions was varied but the sum of the mass of the two

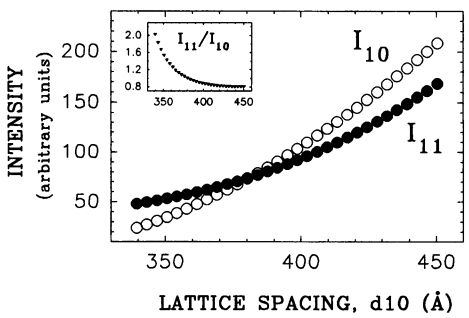

FIGURE 4 Lattice effects. Effect of changing lattice spacing is studied by assuming that as the spacing changes, structures of myosin filaments including cross-bridges and thin filaments remain unchanged. Both I_{10} and I_{11} increase with lattice size increase.

fractions was kept constant and equal to the mass of the whole cross-bridge population.

Fig. 5 *a* demonstrates the change of I_{10} and I_{11} with an increase in azimuthal nonuniformity of the cross-bridge halo. As the number of cross-bridges located along [1,1] lines increases, the I_{11}/I_{10} ratio increases due to the increase in I_{11}; I_{10} changes very little. The increase in I_{11} depends significantly on the angle β. As β approaches 90°, I_{11} becomes progressively less sensitive to the azimuthal nonuniformity of cross-bridge distribution.

2) Quite different behavior of equatorial reflections can be seen if cross-bridges are more concentrated along myosin-myosin [1,0] lines (see Fig. 5 *b*). I_{11} is still very sensitive to the degree of azimuthal sixfold symmetry of cross-bridge distribution, but in this case it decreases with increase in the number of cross-bridges located along [1,0] lines, and I_{10} again remains relatively constant.

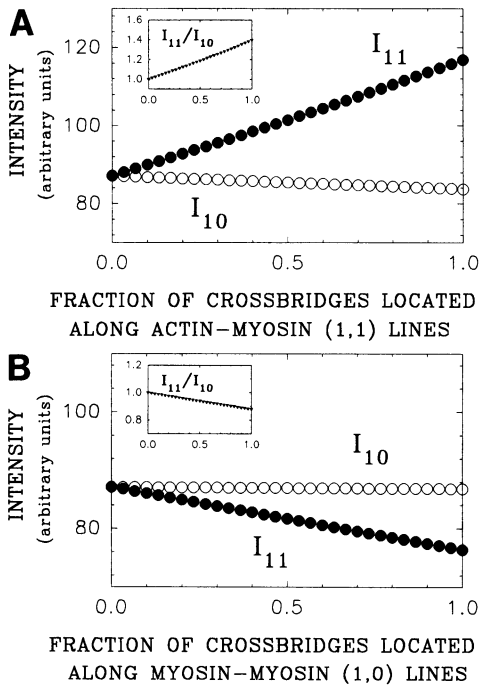

FIGURE 5 Azimuthal uniformity of cross-bridge halo. (*a*) Cross-bridges surrounding thick filaments are assumed to consist of two populations, those that are distributed uniformly around backbone and those located only along actin-myosin lines [1,1]. Both fractions of cross-bridges are assumed to have the same configurations: r_c = 138 Å, α = 55°, and β = 40°. I_{11} increases as cross-bridge density increases along actin-myosin lines, while I_{10} does not change. (*b*) The model is similar to (*a*) except that the cross-bridges of the second fraction located along myosin-myosin lines (1,0). Now I_{11} decreases as cross-bridges concentrate along myosin-myosin lines and I_{10} is stable again.

Varying the population of cross-bridges in the halo surrounding the thick filament

There is evidence (see Lowy and Poulsen, 1987; Lowy et al., 1991) that a fraction of cross-bridges is disordered and varies with changing conditions of muscle.

In our model (Fig. 6) the cross-bridges are assumed to distribute among two populations of cross-bridges. The sum of the masses of two fractions remains constant while the proportion is allowed to vary. One population is the ordered fraction, located around the thick filament backbone, which forms a compact halo of uniform density; the other population is the disordered fraction, consisting of the cross-bridges distributed randomly in all available space between filaments. The latter population does not produce any Bragg reflections but increases the diffuse scattering.

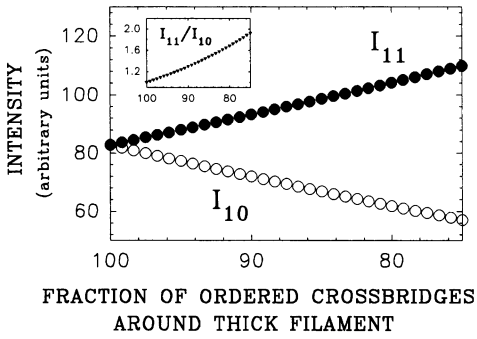

FIGURE 6 Changing the mass of cross-bridge halo. Cross-bridges are considered to consist of two populations, those surrounding thick filaments (ordered fraction) and those distributed randomly in between actin-myosin space (disordered fraction). The disordered fraction does not make any contribution to I_{10} and I_{11} intensities but increases the diffusion scattering and reduces the protein-solution contrast of the cell. I_{10} and I_{11} are very sensitive to the mass of ordered cross-bridge halo and change in a reciprocal way.

The diffraction pattern is calculated from the ordered fraction of cross-bridges with the correction that the disordered part reduces protein-solution contrast. Fig. 6 demonstrates that a decrease from 100 to 75% of mass in the ordered fraction induces a change in I_{11}/I_{10} ratio approximately by a factor of 2. The absolute intensities I_{10} and I_{11} change in a reciprocal way.

DISCUSSION

Modeling studies of equatorial diffraction patterns provide valuable insight into the observed changes in intensities. Analysis of the behavior of intensities I_{10} and I_{11} suggests (and at the same time excludes) various interpretations, even though the modeling does not provide unique solutions. In addition, by modeling one could avoid the uncertainties in choosing phases of reflections needed for Fourier synthesis as well as cutoff effects due to the limited number of observed reflections (Yu, 1989).

The models shown in the previous section illustrate a variety of factors that may affect equatorial intensities. In many cases changes in the intensity I_{10} cannot be considered as a direct indication of mass changes around thick filaments, and changes in I_{11} do not prove an inevitable mass redistribution near the surface of thin filaments.

For the interpretation of diffraction patterns, it is helpful in many cases to consider Fourier transforms of individual components of muscle sarcomere.

Fig.7 *a* shows the scattering amplitudes (Fourier transforms) of the thick filament backbone, $F_B(R)$, and the cross-bridge halo surrounding the backbone, $F_H(R)$, as a function of the radius, R, in reciprocal space calculated for the basic model (see equations in Materials and Methods). Fourier transforms of the thin filament, $F_A(R)$, and the attached cross-bridges, $F_{att}(R)$, are shown in Fig. 7 *b*. Due to the basic properties of Bessel functions, the transform curves are sign-alternating functions in reciprocal space. At the origin, each transform is equal to the relative weights of the corresponding components: W_B, W_H, W_A, W_{att}. The transform amplitudes reach zero at distances inversely dependent on the size of the structures: the greater the real size of the component, the shorter the reciprocal radius R at which the amplitude reaches the first zero.

To see how the observed intensities of the equatorial reflections are determined by the components of the unit cell, it is convenient to draw pairs of curves: $F_B(R) + F_H(R) = F_{Thick}(R)$ with $-[F_A(R) + F_{Att}(R)] = -F_{Thin}(R)$ (Fig.7 *c*) and also $F_B(R) + F_H(R)$ with $2[F_A(R) + F_{Att}(R)] = 2F_{Thin}(R)$ (Fig. 7 *d*). According to Table 1, the sum $F_{Thick}(R) - F_{Thin}(R)$ gives the structural amplitudes of [1,0], [2,0], [2,1], and [3,1] reflections at corresponding distances of R (Fig. 7 *c*) and the sum $F_{Thick}(R) + 2F_{Thin}(R)$ gives the amplitudes of [1,1], [3,0], and [2,2] reflections (Fig. 7 *d*). The observed intensities I_{hk} (Fig. 7 *e*) are equal to the squares of the resulting amplitudes with Lorenz correction (see Materials and Methods).

Consider a few examples of using Fourier transforms:

1) Attachment of cross-bridges. When all cross-bridges leave the thick filament region and attach to the thin fila-

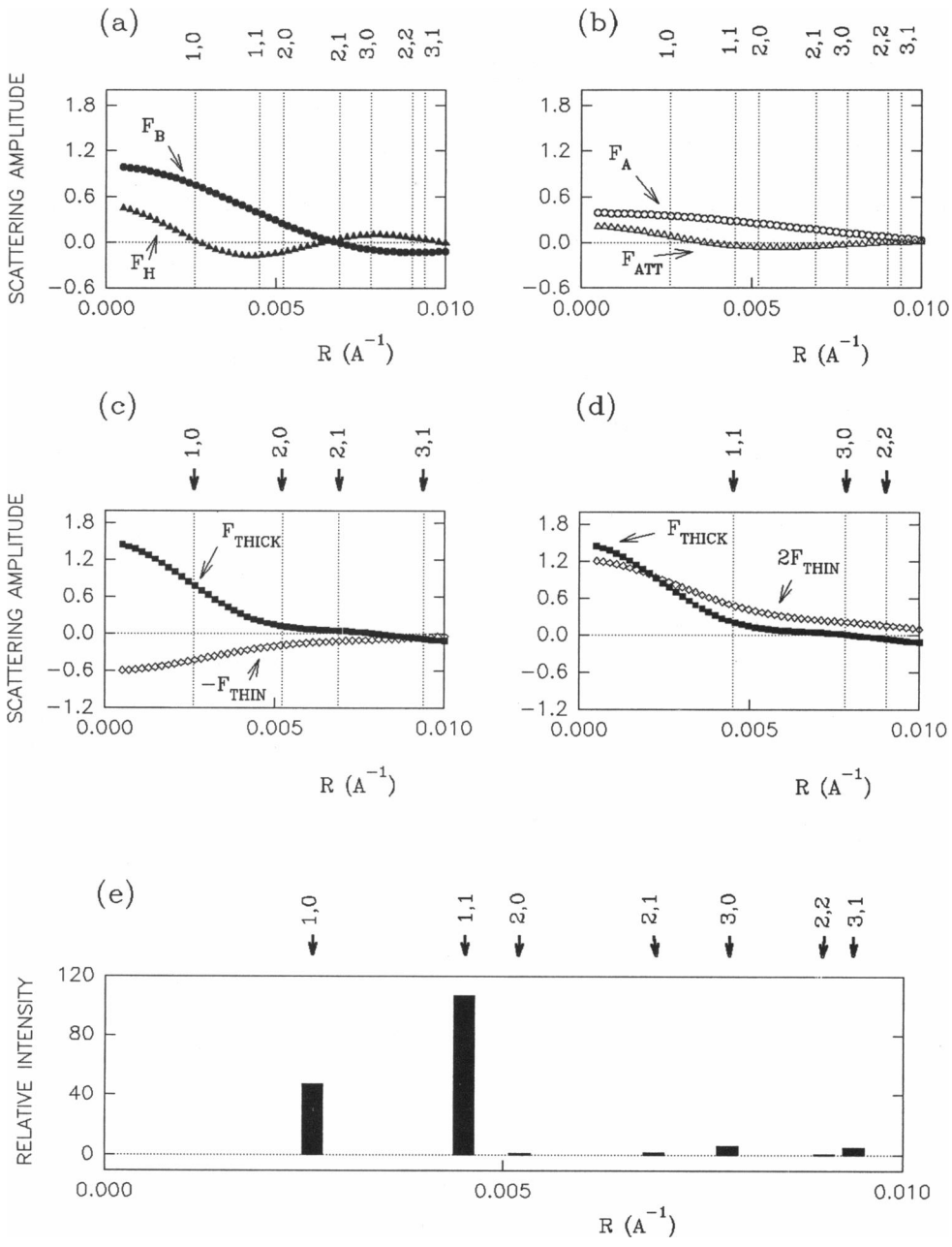

FIGURE 7 Fourier transforms of different components calculated for the "basic" model (see Results) but one-half of the cross-bridges are stereospecifically attached to actin at $\phi_{att} = 45°, \psi_{att} = 60°$. (*a*) Transforms of backbone, F_B, and cross-bridge halo, F_H; (*b*) transforms of thin filament, F_A, with attached cross-bridges, F_{ATT}. (*c* and *d*) $F_{THICK} = F_B + F_H$, $F_{THIN} = F_A + F_{ATT}$. $F_{THICK} - F_{THIN}$ give the scattering amplitudes of [1,0], [2,0], [2,1] and [3,1] reflections at appropriate radii, R, of reciprocal space; $F_{THICK} + 2F_{THIN}$ give the scattering amplitudes of [1,1], [3,0], and [2,2] reflections. (*e*) The relative intensities of corresponding reflections (see Materials and Methods).

ments, they become centered around actin filaments (as in the rigor state). The scattering amplitude $F_{Thick}(R)$ (= $F_B(R)$ + $F_H(R)$) now consists only of the transform of the backbone, $F_B(R)$. Simultaneously, the $F_{Att}(R)$ component of $F_{Thin}(R)$ (= $F_A(R)$ + $F_{Att}(R)$) increases in magnitude. At [1,0] spacing, $F_{Thick}(R)$ changes little, because the magnitude of the transform of the cross-bridge halo $F_H(R)$ was originally very small (see Fig. 7 *a*). Meanwhile, the absolute value of the scattering amplitude $F_{thin}(R)$ increases considerably at [1,0] spacing. Hence, the I_{10} decreases. At [1,1] spacing $F_{Thick}(R)$ increases considerably because $F_H(R)$ becomes zero, while $2F_{Thin}(R)$ decreases slightly, and as a result I_{11} increases (see Fig. 2 *a*). It is interesting to note that the well-known effect of reciprocal changes in I_{10} and I_{11} when cross-bridges attach to and surround actin is mainly caused by an increase of magnitude in $F_{Thin}(R)$ at [1,0] and an increase in $F_{Thick}(R)$ at [1,1].

2) Radial movement of cross-bridge halo. When cross-bridges move from the surface of the thick filament backbone toward the thin filament, the Fourier transform of the cross-bridge, $F_H(R)$ (Fig. 7 *a*), shifts toward the origin in the reciprocal space without changing amplitude. Normally, the radial movement of cross-bridges within a muscle is restricted to the area between thick and thin filaments. Such limited movements cause more significant alteration of the transform at [1,0] than that at [1,1], since $F_H(R)$ has a steep slope at [1,0] but a plateau at [1,1] (see also Fig. 2 *c*).

3) Random isotropic displacement of filaments. If the thick filaments are displaced randomly from their lattice points in a cross section, their projected densities might appear as if the thick filaments are "smeared" to a larger diameter. This will cause a shift of $F_{Thick}(R)$ leftward in the reciprocal space, and the values of $F_{Thick}(R)$ will decrease at spacings of [1,0] and [1,1]. Hence, both I_{10} and I_{11} will decrease.

If the thin filaments become disordered, a similar shift will occur to $F_{Thin}(R)$ and the magnitude will decrease at [1,0] and [1,1] spacings. As a result I_{10} will increase and I_{11} will decrease. Therefore, disorder in the thin filament distribution will make the diffraction pattern appear more like that of relaxed muscle.

4) Changes in attachment mode. If the angle of cross-bridge attachment increases, the apparent outer diameter of the projection of the cross-bridges increases. $F_{Att}(R)$ will shift leftward, and accordingly the absolute value of $F_{Att}(R)$ at [1,0] decreases, while the absolute value of $F_{Att}(R)$ at [1,1] increases (Fig. 7 *b*). These changes result in increasing I_{10} and decreasing I_{11} (see also Fig. 2 *b*).

Sensitivity of parameters on Fourier transforms

One question concerning the models is how much of their behavior depends on their specific features, e.g., sizes and shapes. The behavior of the models will be qualitatively the same if the transforms of their individual structures (i.e., backbone, cross-bridges; see Fig. 7) conserve the same characteristic features (phases and amplitudes in the particular areas) regardless of variations in size and shape. Consider one example. To describe the density of the cross-bridge halo we used the axial projection of individual cross-bridge represented by a set of equal overlapping spheres in a straight line. Recent studies (Rayment et al., 1993) showed that the shape of myosin head (S-1) looks more like a flexed pear. To study the influence of the shape of S-1 on the transform we simulated Rayment's (Rayment et al., 1993) S-1 structure by spheres of different radii as shown on Fig. 8. In this case, Fourier transforms calculated for cross-bridge halos with two different shapes of S-1 show no significant distinctions in the reciprocal area up to 0.01 Å^{-1}.

In general, at low diffraction angles the transforms of thick and thin filaments do not depend on fine features of original structures. We can expect that the behavior of more structurally detailed models will be qualitatively the same as described in the present study.

A strategy in interpretating the changes observed in equatorial diffraction pattern

Individual intensities

Model studies demonstrate that the ratio I_{11}/I_{10} changes not only when cross-bridges attach to thin filaments (as often believed); rather, there are other factors that also can induce changes of the same magnitude. To distinguish various causes, the first measure is to follow the individual intensities, particularly I_{10} and I_{11} rather than the ratio I_{11}/I_{10}. For example, one can distinguish the radial movement of cross-bridge halo from other possibilities by observing the characteristic increase/decrease of I_{10}, as compared with I_{11},

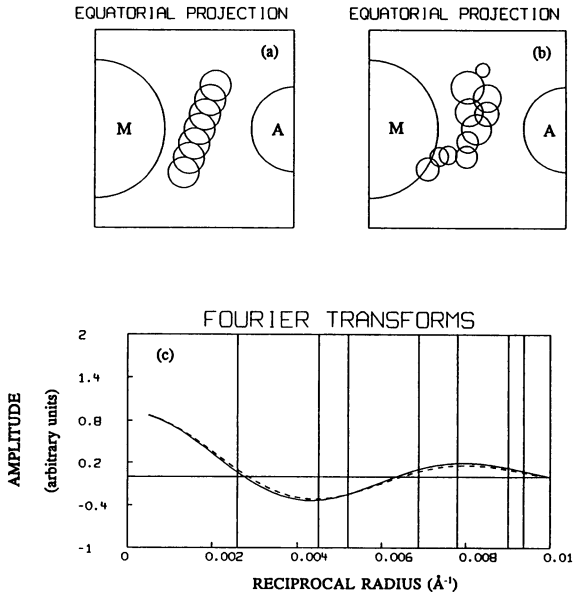

FIGURE 8 Fourier transforms calculated for cross-bridge halos with different shapes of S-1. (——) Transform for S-1 represented by seven overlapping spheres in a straight line. (- - - - - -) Transform for S-1 simulating at low resolution the structure found by Rayment et al. (1993). At low angles of diffraction (up to 0.01 Å^{-1}) two transforms differ only slightly.

which changes very little (Fig. 2 *c*). If only the thick filaments are disordered while the thin filaments remain in ideal lattice positions, the effect on the diffraction pattern (Fig. 3 *a*) is similar to radial movement of cross-bridges. It should be pointed out, however, that if there is considerable disordering in the sarcomere, the thin filaments would be disordered at least as much as the thick filaments (or more) because the thin filaments are thinner and more flexible than the thick filaments. With disordering of both types of filaments at the same time, I_{11} will decrease even more than I_{10} (see Fig. 3 *c*). Thus, the insensitivity of I_{11} appears to be characteristic of the radial movement of cross-bridge mass from the backbone.

The models of azimuthal redistribution of cross-bridge density also demonstrate a characteristic behavior of the diffraction patterns: I_{10} is rather insensitive while I_{11} increases as cross-bridges concentrate along myosin-actin lines (Fig. 5 *a*), or decreases when cross-bridges concentrate along myosin-myosin lines (Fig. 5 *b*). The latter is similar to the case where both types of filaments undergo a disordering effect when the thin filaments are more disordered (see Fig. 3 *c*).

Comparing individual intensities requires careful normalization procedures, because they are directly affected by camera conditions, absorption by the bathing media, and the size of the specimen. Procedures using a single reflection (e.g., I_{10}) obtained under one condition as the normalization factor have been shown to be effective (Yu and Brenner, 1989).

Models showing the reciprocal change of I_{10} and I_{11} (e.g., changing the fraction of ordered cross-bridges (Fig. 6), varying the number of attached cross-bridges (Fig. 2 *a*) or the disordering of actin filaments (Fig. 3 *b*) are difficult to distinguish. One possible means of further analysis is to compare higher orders of the equatorial patterns.

Higher orders of equatorial reflections

Higher orders of the equatorial reflections can supply information that can help to exclude, or at least provide additional evidence in favor of, some particular models. For example, analysis of higher orders can reveal azimuthal redistributions of cross-bridge density resulting in appearance of 6-fold cylindrical symmetry in the halo. As a rule, the azimuthal nonuniformity of the density of the cross-bridge halo causes one, or more, higher-order reflections to increase considerably in intensity depending on the azimuthal orientation of density maxima and radial width (Fig. 9 *a*). In the case where the filament lattice becomes disordered, all higher orders of equatorial reflections decrease in intensity significantly (Fig. 9 *b*).

Other measures to aid interpretation

In many cases even analysis of higher orders cannot distinguish different parameter changes. For example, when a fraction of the cross-bridges leaves the vicinity of thick filaments and becomes a part of disordered population within the lattice, or when a fraction of cross-bridges attaches to thin filaments, there are similar changes in the intensities of higher orders. However, an increase in the disordered fraction of cross-bridges results in an increase of incoherent scattering

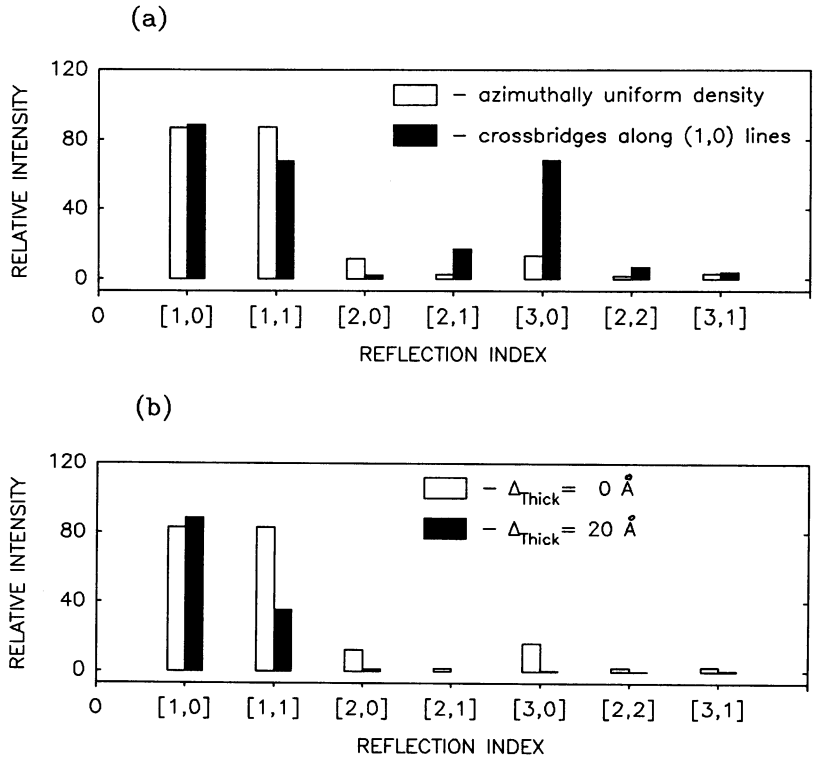

FIGURE 9 Calculated intensities of higher order equatorial reflections. (*a*) Density of cross-bridge halo increases along myosin-myosin lines (corresponds to the model in Fig. 5 *b*). (*b*) Thick and thin filaments are assumed to be subject to random displacement from their idealized positions in the lattice (corresponds to the model in Fig. 3 *c*, $\Delta_{Thin} = 1.6\Delta_{Thick}$). In both models I_{10} and I_{11} change in the same way but higher orders are different.

and the diffuse background increases (Lowy and Poulsen, 1990; Lowy et al., 1991).

Effects of filament disordering are generally accompanied by width changes of equatorial reflection peaks (Yu et al., 1985).

Changes in filament lattice spacing can induce significant changes in equatorial intensities without any mass redistribution inside the sarcomere. To minimize such complications, one could apply, e.g., osmotic pressure to keep the filament lattice spacing constant (Brenner and Yu, 1993).

CONCLUSION

Using a simplified model of the filament lattice, we have demonstrated that various factors, in addition to cross-bridge attachment to actin, can affect the equatorial intensities, particularly I_{10} and I_{11}. A great deal of information could be lost if only the intensity ratio were studied as an indication of cross-bridge attachment.

Several general features of our findings can be summarized as follows:

1) If I_{10} changes while I_{11} is relatively stable, it is very likely that there is radial movement of the cross-bridge halo surrounding the thick filaments (Fig. 2 *c*).

2) If I_{11} changes while I_{10} is relatively stable, there is probably azimuthal nonuniform redistribution of cross-bridge density (Fig. 5, *a* and *b*), provided that there is a significant increase in the intensities of some high order reflections. Alternatively, disordering of filament lattice (Fig. 3 *c*) is indicated if all higher orders of equatorial reflections decrease in intensity and (possibly) increase in the widths of reflections.

3) If I_{10} and I_{11} change in a reciprocal way, it could be an indication of attachment of cross-bridges to actin as in the rigor case (Fig. 2 *a*), changing of the axial attachment angles of cross-bridges already bound to actin (Fig. 2b), or disordering of cross-bridges located in the halo surrounding the thick filaments (Fig. 6).

4) If I_{10} and I_{11} change significantly in the same direction, it could be an indication of the change in the filament lattice spacing (Fig. 4) or if all the reflections including the higher orders change in widths it is an indication of considerable ordering/disordering of the filament lattice.

REFERENCES

Brenner, B., and L. C. Yu. 1985. Equatorial x-ray diffraction from single skinned rabbit psoas fibers at various degrees of activation. Changes in intensities and lattice spacing. *Biophys. J.* 48:829–834.

Brenner, B., and L. C. Yu. 1993. Structural changes in the actomyosin cross-bridges associated with force generation. *Proc. Natl. Acad. Sci. USA.* 90:5252–5256.

Brenner, B., L. C. Yu, and R. Podolsky. 1984. X-ray diffraction evidence for cross-bridge formation in relaxed muscle fibers at various ionic strengths. *Biophys. J.* 46:299–306.

Cecchi, G., P. J. Griffiths, M. A. Bagni, C. C. Ashley, and Y. Maeda. 1991. Time-resolved changes in equatorial x-ray diffraction and stiffness during rise of tetanic tension in intact length-clamped single muscle fibers. *Biophys. J.* 59:1273–1283.

Haselgrove, J. C., M. Steward, and H. E. Huxley. 1976. Cross-bridge movement during muscle contraction. *Nature.* 261:606–608.

Huxley, H. E. 1968. Structural difference between resting and rigor muscle: evidence from intensity changes in the low equatorial x-ray diagram. *J. Mol. Biol.* 37:507–520.

Huxley, H. E. 1978. Time resolved x-ray diffraction studies on muscle. *In*: International Symposium on the Current Problems of Sliding Filament Model and Muscle Mechanics. H. Sugi and G. Pollack, editors. University of Tokyo Press, Tokyo.

Huxley H. E., M. Kress, A. F. Faruqi, and R. M. Simmons. 1988. X-ray diffraction studies on muscle during rapid shortening and their implications concerning crossbridge behaviour. *Adv. Exp. Med. Biol.* 226:347–352.

Huxley, H. E., R. M. Simmons, A. R. Faruqi, M. Kress, J. Bordas, and M. H. J. Koch. 1983. Changes in the x-ray reflections from contracting muscle during rapid mechanical transients and their structural implications. *J. Mol. Biol.* 169:469–506.

Irving, M., V. Lombardi, G. Piazzesi, and M. A. Ferenczi. 1992. Myosin head movements are synchronous with the elementary force-generating process in muscle. *Nature.* 357:156–158.

Irving, T. C., and B. M. Millman. 1989. Changes in thick filament structure during compression of the filament lattice in relaxed frog sartorius muscle. *J. Muscle Res. Cell Motil.* 10:385–394.

Lowy, J., D. Popp, and A. A. Stewart. 1991. X-ray studies of order-disorder transitions in the myosin heads of skinned rabbit psoas muscles. *Biophys. J.* 60:812–24.

Lowy, J., and F. R. Poulsen. 1987. X-ray study of myosin heads in contracting frog skeletal muscle. *J. Mol. Biol.* 194:595–600.

Lowy, J., and F. R. Poulsen. 1990. Studies of the diffuse x-ray scattering from contracting frog skeletal muscles. *Biophys. J.*57:977–985.

Lymn, R. W. 1978. Myosin subfragment-1 attachment to actin: expected effect on equatorial reflections. *Biophys. J.* 21:93–98.

Lymn, R. W., and G. H. Cohen. 1975. Equatorial x-ray reflections and cross arm movement in skeletal muscle. *Nature.* 258:770–772.

Malinchik, S., and L. Yu. 1993. Analysis of factors that affect equatorial x-ray diffraction from skinned rabbit muscle fibers. *Biophys. J.* 64:26*a* (Abstr.).

Miller, A., and R. T. Tregear. 1972. Structure of insect fibrillar flight muscle in the presence and absence of ATP. *J. Mol. Biol.* 70:85–104.

Podolsky, R. J., H. Onge, L. Yu, and R. W. Lymn. 1976. X-ray diffraction of actively shortening muscle. *Proc. Natl. Acad. Sci. USA.* 73:813–817.

Poole, K. J., G. Rapp, Y. Maeda, R. S. Goody. 1988. The time course of changes in the equatorial diffraction patterns from different muscle types on photolysis of caged-ATP. *Adv. Exp. Med. Biol.* 226:391–404.

Rayment, I., W. R. Rypniewski, K. Schmidt-Base, R. Smith, D. R. Tomchick, M. M. Benning, D. A. Winkelmann, G. Wesenberg, and H. M. Holden. 1993. Three-dimensional structure of myosin subfragment-1: a molecular motor. *Science.* 261:50–58.

Sherwood, D. 1976. Crystals, X-Rays and Proteins. Wiley, New York.

Squire, J. M. 1981. The structural basis of muscle contraction. Plenum Press, London.

Vainstein, B. K. 1966. Diffraction of x-rays by chain molecules. Elsevier, Amsterdam.

Yagi, N., S. Takemori, and M. Watanabe. 1993. An x-ray diffraction study of frog skeletal muscle during shortening near the maximum velocity. *J. Mol. Biol.* 231:668–77.

Yu, L. C. 1989. Analysis of equatorial x-ray diffraction patterns from skeletal muscle. *Biophys. J.* 55:433–440.

Yu, L. C., and B. Brenner. 1989. Structures of actomyosin crossbridges in relaxed and rigor muscle fibers. *Biophys. J.* 55:441–453.

Yu, L., J. Hartt, R. Podolsky. 1979. Equatorial x-ray intensities and isometric force levels in frog sartorius muscle. *J. Mol. Biol.* 132:53–67.

Yu, L. C., A. C. Steven, G. R. S. Naylor, R. C. Gamble, and R. J. Podolsky. 1985. Distribution of mass in relaxed frog skeletal muscle and its redistribution upon activation. *Biophys. J.* 47:311–321.